Memoirs of the Faculty of Engineering, Okayama University, Vol.30, No. 1, pp.89-97, December 1995

Electronic Structure of Mixed Perovskite Oxides

Chieko TOTSUJI*, Yoshiaki SANAKA*, and Hiroo TOTSUJI*

(Received October 2 , 1995)

Based on the tight-binding method, electronic bands of the mixed perovskite oxides are calculated in order to develop the electronic theory of ferroelectric phase transitions in these mixtures which are difficult to describe within the phenomenological theories. Diagonal elements of Hamiltonian matrix of parent materials are assumed to differ by 0.1eV and mixtures are simulated by lattices of supercells containing $2^3 = 8$ or $3^3 = 27$ unit cells randomly assigned to either material. The width of the conduction and valence bands have maxima and the band gap has a minimum at intermediate mixing ratio. Results are in agreement with those of other analyses on random systems and even 2^3-cell computation seems to serve as a first approximation for our purpose.

I. Introduction

The perovskite oxides are known to cover a wide variety of materials, including dielectrics, conductors, and superconductors, depending on constituent metallic ions. Barium titanate ($BaTiO_3$), lead titanate ($PbTiO_3$), and potassium niobate ($KNbO_3$) are well-known examples of perovskite oxide dielectrics.

Barium titanate undergoes successive phase transitions; from high to low temperatures, it takes cubic, tetragonal, orthorhombic, and rhombohedral structures, being a ferroelectric in the latter three. Potassium niobate has also successive phase transitions, while lead titanate has only one phase transition.

When $BaTiO_3$ is mixed with $PbTiO_3$, the transition temperature to the ferroelectric phase increases with the concentration of the latter monotonously. When only a small amount of $KNbO_3$ is added to $BaTiO_3$, however, the transition temperature decreases drastically and we have a minimum at intermediate mixing ratios as shown in Fig.1. We have also other examples in which properties of mixtures are very sensitive to small changes in concentrations and far from the average of parent materials.

*Department of Electrical and Electronic Engineering

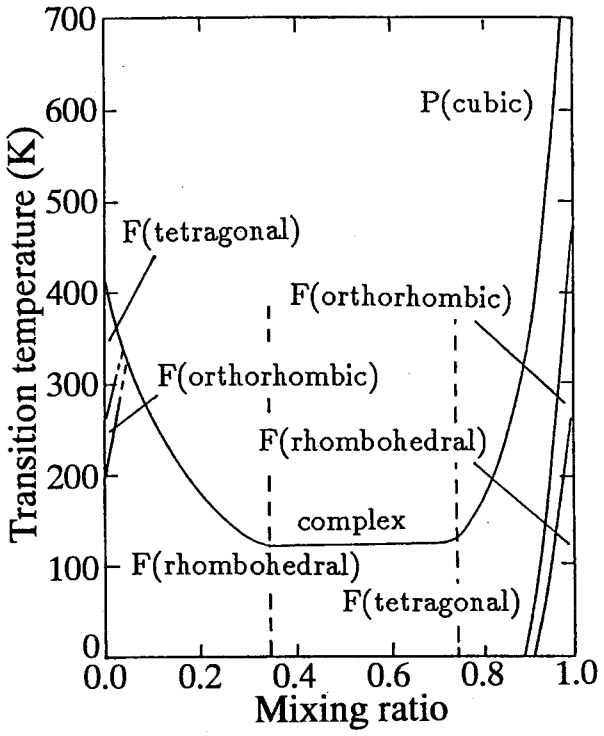

Fig.1. Phase diagram of $(1-x)BaTiO_3 \cdot xKNbO_3$.[7)]

The phenomenological theory cannot explain these peculiar properties of mixed crystals of perovskites and we need a theory based on the analysis of electronic states in these materials. One of the present authors (C. T.) and T. Matsubara have recently developed an electronic theory for perovskite oxides and succeeded in describing induced ferroelectric transitions of some quantum-paraelectrics.[1,2)] They have also predicted a sudden decrease of transition temperature in mixed perovskites employing a model calculation of electronic bands.[3)]

The mixed material has a stochastic nature and its electronic structure is affected by randomness: The electronic bands are usually broadened and the energy gap becomes narrower in comparison with pure materials. Based on the known results of the coherent potential approximation,[4)] they have assumed the modification of band structure due to randomness in mixed crystals and estimated the change of transition temperatures. The ferroelectric transition temperature depends critically on the balance between the broadening of electronic bands and narrowing of band gap. The results indicate that the ferroelectric transition temperature is decreased rapidly by mixing when the effect of the broadening of band width exceeds that of the narrowing of band gap. The purpose of this paper is to investigate the electronic band structure in mixed perovskite-type oxide crystals constructing lattices of supercells as a model of random mixtures.

II. Energy Bands of the Perovskite Oxide

It has been reported that electronic structures of perovskite oxides are described to a good accuracy by the tight-binding approximation which takes a metallic ion and surrounding six oxygen ions in a configuration of body-centered octahedron.[5,6] An example of the band structure of $SrTiO_3$ and the density of states is displayed in Fig.2.

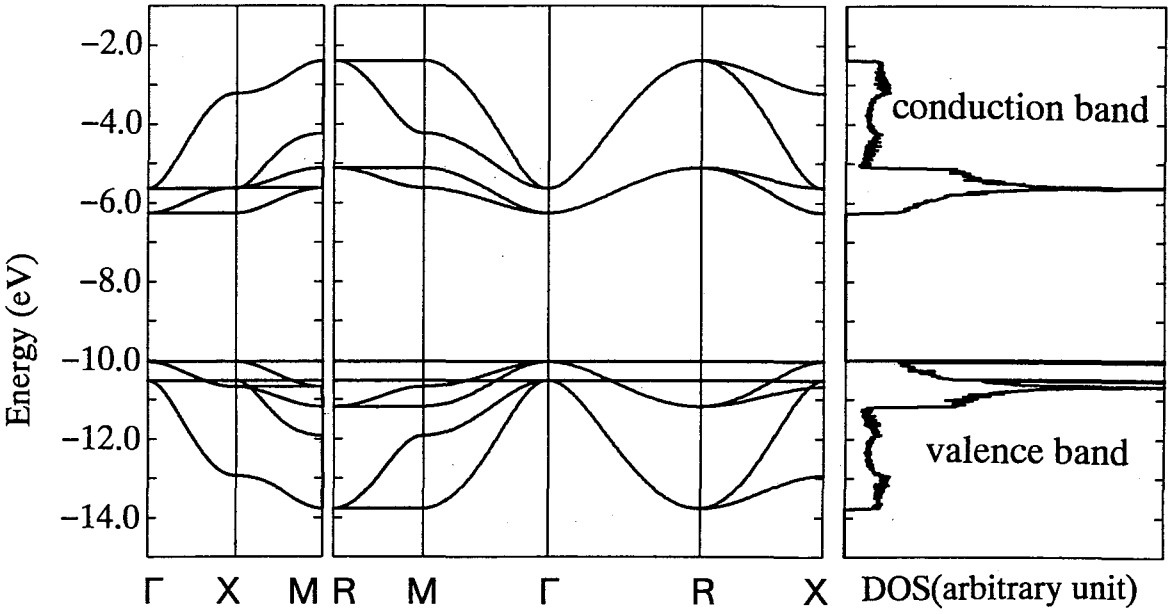

Fig.2. Electronic band structure of $SrTiO_3$ based on tight binding approximation.

The conduction bands are mainly composed of *d*-orbitals from the metallic ion at the body-center site and the valence bands, of *p*-orbitals from oxygen ions. The tight-binding parameters are taken from Reference 6 and here we take only the nearest-neighbor *p-d* interactions into account. While next-nearest-neighbor *p-p* interactions remove the high degeneracy in the upper valence bands, the overall behavior of the density of states can be reproduced without them and we confine ourselves within nearest-neighbor interactions at this stage.

III. Band Calculation for Mixed Perovskite Oxides

As a simple model of mixed crystal of perovskite-type oxides ABO_3 and $A'B'O_3$, we take a lattice of supercells composed of many unit cells which are randomly assigned to the unit cell of either ABO_3 or $A'B'O_3$ in accordance with the mixing ratio. Though this model obviously has a long range order of superlattice, we may have some insight into the density of states of mixtures by increasing the scale of the superlattice. In this paper, the superlattices containing $2^3 = 8$ unit cells and $3^3 = 27$ unit cells are considered.

We assume that one of parent materials has the same band parameters as $SrTiO_3$. As randomness, we take into account those in the diagonal parts of the Hamiltonian matrix, atomic term values of *d*-orbital electron of B-site ion and *p*-orbital electron of oxygen ion. The off-diagonal part contains the overlap integrals between adjacent ions. For nearest neighbor interactions, they depend on the ionic radius of the B-site ion and the interatomic distance

between B-site ion and oxygen ion. In the case where the lattice constants of two pure materials are very close to each other and/or B-site ion is the same, we can neglect the randomness in the off-diagonal part. The whole superlattice Hamiltonian of a 8-cell crystal is given in Appendix. A band structure obtained by a 8-cell superlattice calculation for pure $SrTiO_3$ is shown in Fig.3. Note the (apparent) difference in the based structure from that in Fig.2 coming from the reduced size of the Brillouin zone. An example of (imaginary) mixture of $\frac{3}{8}(SrTiO_3) \cdot \frac{5}{8}(SrTiO_3)'$ is shown in Fig.4. The atomic values of $(SrTiO_3)'$ are lowered by 1.0 eV.

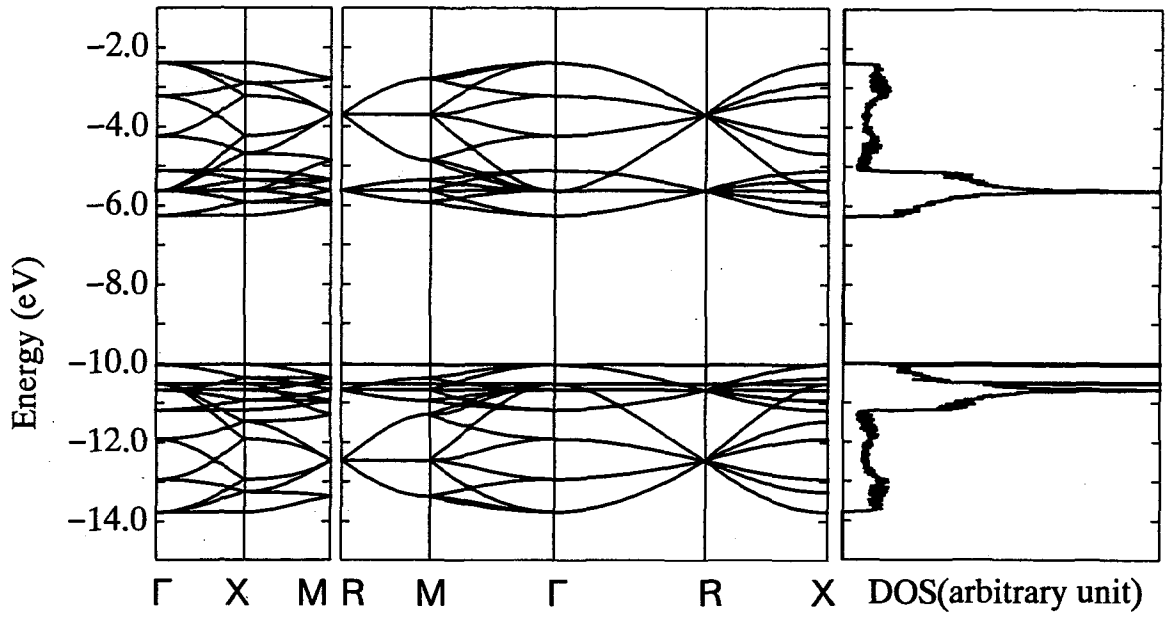

Fig.3. Electronic band structure of $SrTiO_3$ using 2^3-cell superlattice.

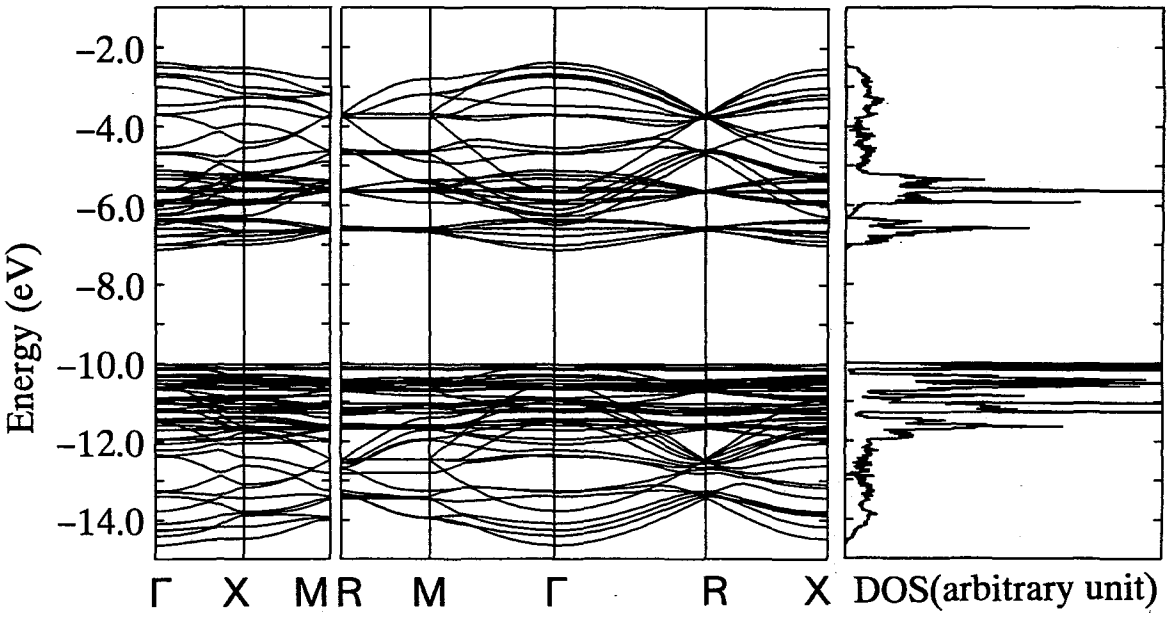

Fig.4. Electronic energy band structure of $\frac{3}{8}(SrTiO_3) \cdot \frac{5}{8}(SrTiO_3)'$.
In $(SrTiO_3)'$, atomic values are reduced by 1.0 eV from that of $(SrTiO_3)$.

With the 8-cell superlattice, we obtain the band structure at the mixing ratios of 0:8, 1:7, 2:6, 3:5, 4:4, 5:3, 6:2, 7:1 and 8:0. There are some possibilities for combinations of positions of unit cells containing impurities: For example, in the case of the ratio of 1:7, all such configurations are equivalent and give the same band structure, while some of 28 configurations possible for the ratio of 2:6 are not equivalent. Taking the average over all possible configurations, we evaluate the band widths and the band gap at each mixing ratio.

In the case of 27-cell superlattice, we have a large number of possible configurations and it is not practical to take them all into account. We therefore compute the average over twenty randomly chosen configurations for each value of mixing ratios $n : 27 - n$, $n = 1, 2, \ldots, 26$.

IV. Results and Discussion

In Figs.5(a), (b), and (c), we show an example of the band gap and the band widths of the mixture of two perovskite oxides obtained by our superlattice analysis. The host material has the parameters of $SrTiO_3$ and diagonal energies of the impurity are assumed to be lowered by 0.1eV. We have used the uppermost values and lowermost values of two electronic bands and obtained the band widths and energy gaps as the difference between average of these values. Filled circles and open circles denote the results of 27-cell and 8-cell computations, respectively.

The 8-cell and 27-cell computations give almost the same results both in band gap and in band widths. In the results of valence band width and band gap, however, we observe small discrepancies between two computations when the concentration of impurity is very close to unity. In this case small amount of host materials gives an isolated level with small density atop of bulk valence band and the valence band width and the band gap are thus overestimated and underestimated, respectively, in Fig.5 where only the position of levels are taken into account. The density of states in this situation is displayed in Fig.6. The critical temperatures of ferroelectric transitions are naturally related to the density of states[3] and these discrepancies may not lead to difficulty.

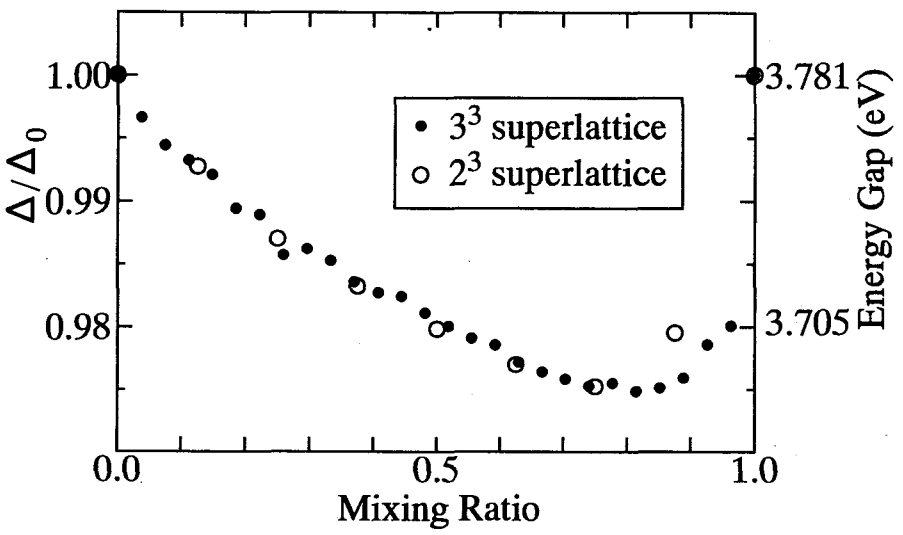

Fig.5(a). Band gap vs. mixing ratio x in $(1-x)(SrTiO_3) \cdot x(SrTiO_3)'$. Atomic values of $(SrTiO_3)'$ are lowered by 0.1 eV from that of $(SrTiO_3)$.

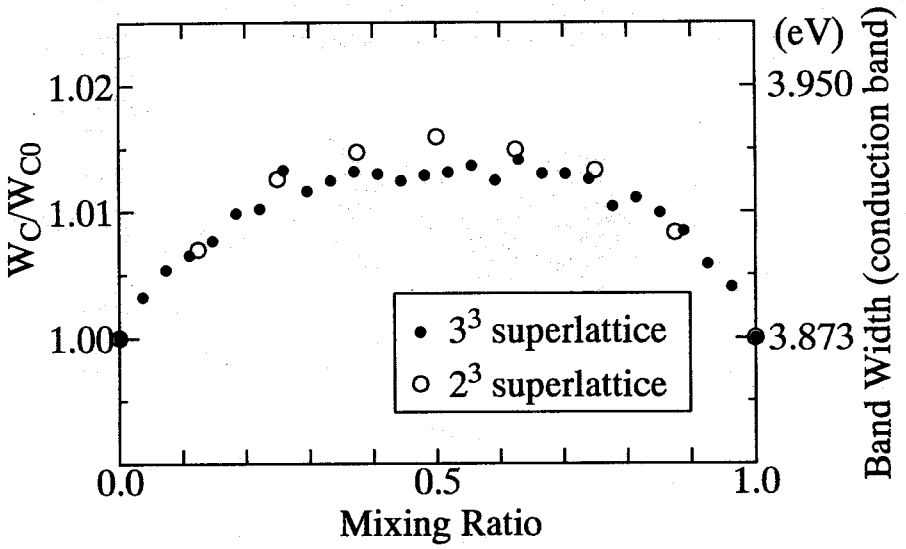

Fig.5(b). Conduction band width vs. mixing ratio x in $(1-x)(SrTiO_3)\cdot x(SrTiO_3)'$. Atomic values of $(SrTiO_3)'$ are lowered by 0.1 eV from that of $(SrTiO_3)$.

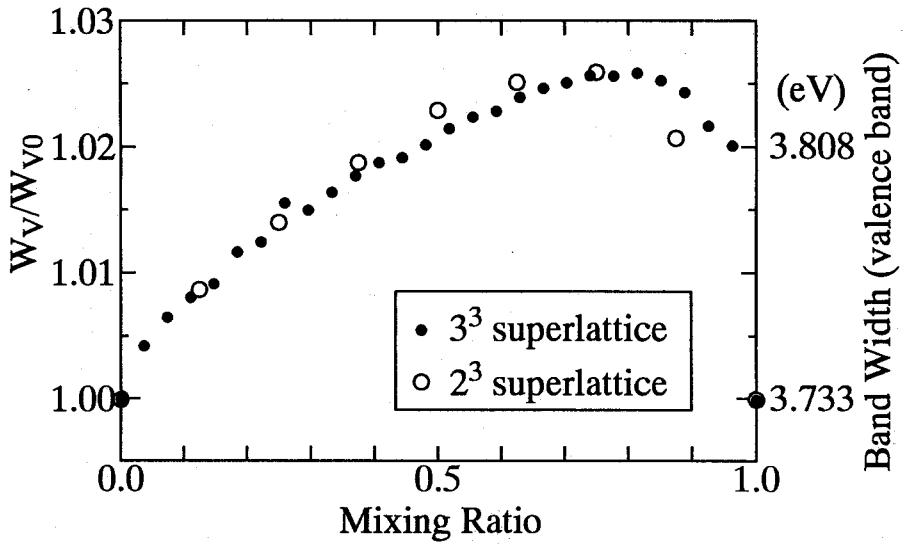

Fig.5(c). Valence band widths vs. mixing ratio x in $(1-x)(SrTiO_3)\cdot x(SrTiO_3)'$. Atomic values of $(SrTiO_3)'$ are lowered by 0.1 eV from that of $(SrTiO_3)$.

The values shown in Fig.5 are averages over various configurations at the same mixing ratio and they fluctuate from one configuration to another. The fluctuations, however, seems to be sufficiently small: The maximum fluctuation in the 27-cell computation is less than 0.003eV.

These results indicate that band widths are increased and the band gap are decreased by mixing similar materials with differences in the diagonal parts of the Hamiltonian matrices. Band widths and band gap have maximum and minimum, respectively, at intermediate mixing ratio. Supercell computations thus provide us with the information for the electronic theory of ferroelectric phase transistions.

As for band widths and band gap, smaller supercells seem to serve as a first approximation. As mentioned earlier, however, superlattices are not random structures in a strict sense. In this respect, larger superlattices may have to be analyzed. The computation with $4^3 = 64$ cell now in progress and details of the analysis of the transition temperature will be reported elsewhere.

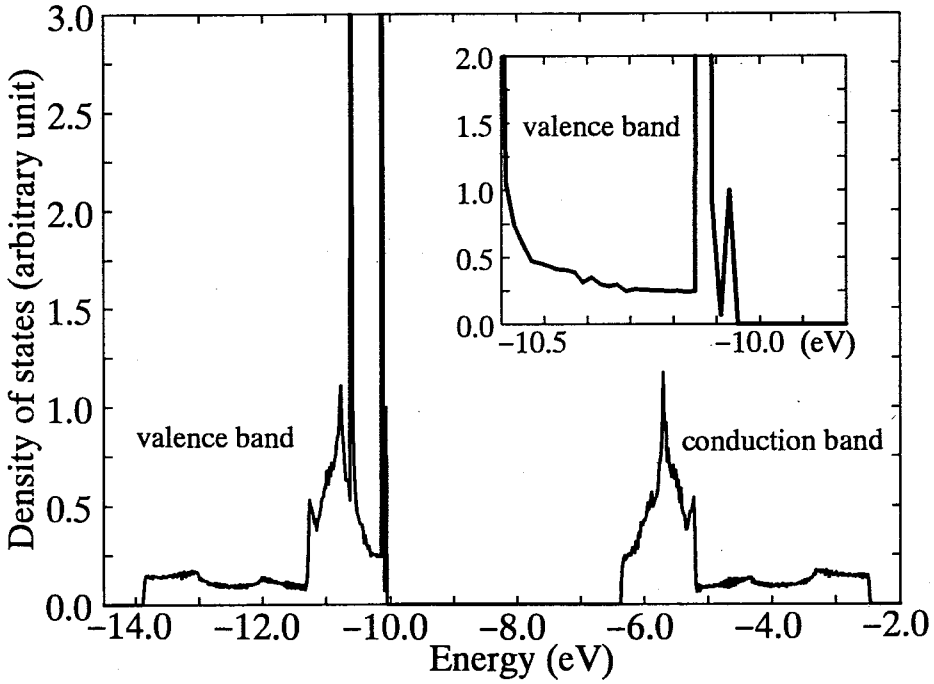

Fig.6. Density of states of $\frac{1}{27}(SrTiO_3) \cdot \frac{26}{27}(SrTiO_3)'$. Atomic values of $(SrTiO_3)'$ are reduced by 0.1 eV from that of $(SrTiO_3)$. Detailed density of states of upper valence band is shown in inset.

Acknowledgements

One of the authors (C. T.) would like to express her thanks to Professor Takeo Matsubara for encouragements and discussions. This work has been partly supported by the Murata Science Foundation.

Appendix. Superlattice Hamiltonian ($2 \times 2 \times 2$).

For the unit cell with a metal ion at the body center and three oxygen ions at the face centers, electronic Hamiltonian is given by a 14×14 matrix as follows.

$$\mathsf{M}_0 = \begin{pmatrix} \mathsf{M}_{xyz} & 0 & 0 & 0 \\ 0 & \mathsf{M}_{yz} & 0 & 0 \\ 0 & 0 & \mathsf{M}_{zx} & 0 \\ 0 & 0 & 0 & \mathsf{M}_{xy} \end{pmatrix},$$

where

$$\mathsf{M}_{xyz} = \begin{pmatrix} \varepsilon_{\mathrm{d}\varepsilon} & 0 & \frac{1}{2}V_{\mathrm{pd}\sigma}\left(\mathrm{e}^{ik_xd} - \mathrm{e}^{-ik_xd}\right) \\ 0 & \varepsilon_{\mathrm{d}\varepsilon} & -\frac{\sqrt{3}}{2}V_{\mathrm{pd}\sigma}\left(\mathrm{e}^{ik_xd} - \mathrm{e}^{-ik_xd}\right) \\ \frac{1}{2}V_{\mathrm{pd}\sigma}\left(\mathrm{e}^{-ik_xd} - \mathrm{e}^{ik_xd}\right) & -\frac{\sqrt{3}}{2}V_{\mathrm{pd}\sigma}\left(\mathrm{e}^{-ik_xd} - \mathrm{e}^{ik_xd}\right) & \varepsilon_{\mathrm{p}\|} \\ \frac{1}{2}V_{\mathrm{pd}\sigma}\left(\mathrm{e}^{-ik_yd} - \mathrm{e}^{ik_yd}\right) & \frac{\sqrt{3}}{2}V_{\mathrm{pd}\sigma}\left(\mathrm{e}^{-ik_yd} - \mathrm{e}^{ik_yd}\right) & 0 \\ -V_{\mathrm{pd}\sigma}\left(\mathrm{e}^{-ik_zd} - \mathrm{e}^{ik_zd}\right) & 0 & 0 \end{pmatrix}$$

$$\begin{pmatrix} \frac{1}{2}V_{\mathrm{pd}\sigma}\left(\mathrm{e}^{ik_yd} - \mathrm{e}^{-ik_yd}\right) & -V_{\mathrm{pd}\sigma}\left(\mathrm{e}^{ik_zd} - \mathrm{e}^{-ik_zd}\right) \\ \frac{\sqrt{3}}{2}V_{\mathrm{pd}\sigma}\left(\mathrm{e}^{ik_yd} - \mathrm{e}^{-ik_yd}\right) & 0 \\ 0 & 0 \\ \varepsilon_{\mathrm{p}\|} & 0 \\ 0 & \varepsilon_{\mathrm{p}\|} \end{pmatrix},$$

and

$$\mathsf{M}_{\alpha\beta} = \begin{pmatrix} \varepsilon_{\mathrm{d}\gamma} & V_{\mathrm{pd}\pi}\left(\mathrm{e}^{-ik_\alpha d} - \mathrm{e}^{ik_\alpha d}\right) & V_{\mathrm{pd}\pi}\left(\mathrm{e}^{-ik_\beta d} - \mathrm{e}^{ik_\beta d}\right) \\ V_{\mathrm{pd}\pi}\left(\mathrm{e}^{ik_\alpha d} - \mathrm{e}^{-ik_\alpha d}\right) & \varepsilon_{p\perp} & 0 \\ V_{\mathrm{pd}\pi}\left(\mathrm{e}^{ik_\beta d} - \mathrm{e}^{-ik_\beta d}\right) & 0 & \varepsilon_{p\perp} \end{pmatrix},$$

$\alpha,\ \beta = x,\ y,\ z.$

The parameters are given by[5)]

$\varepsilon_{\mathrm{p}\|} = -10.519$ eV, $\varepsilon_{\mathrm{p}\perp} = -10.039$ eV, $\varepsilon_{\mathrm{d}\gamma} = -5.638$ eV, $\varepsilon_{\mathrm{d}\epsilon} = -6.258$ eV,

$V_{\mathrm{pd}\pi} = 0.84$ eV, and $V_{\mathrm{pd}\sigma} = -2.1$ eV.

When we label eight unit cells as in Fig.A1, the 8-cell superlattice Hamiltonian takes the form

$$\mathsf{M}_{2\times2\times2} = \begin{pmatrix} \mathsf{M}_1 & \mathsf{S}_x & 0 & \mathsf{S}_y & \mathsf{S}_z & 0 & 0 & 0 \\ \mathsf{S}_x^* & \mathsf{M}_2 & \mathsf{S}_y & 0 & 0 & \mathsf{S}_z & 0 & 0 \\ 0 & \mathsf{S}_y^* & \mathsf{M}_3 & \mathsf{S}_x & 0 & 0 & \mathsf{S}_z & 0 \\ \mathsf{S}_y^* & 0 & \mathsf{S}_x^* & \mathsf{M}_4 & 0 & 0 & 0 & \mathsf{S}_z \\ \mathsf{S}_z^* & 0 & 0 & 0 & \mathsf{M}_5 & \mathsf{S}_x & 0 & \mathsf{S}_y \\ 0 & \mathsf{S}_z^* & 0 & 0 & \mathsf{S}_x^* & \mathsf{M}_6 & \mathsf{S}_y & 0 \\ 0 & 0 & \mathsf{S}_z^* & 0 & 0 & \mathsf{S}_y^* & \mathsf{M}_7 & \mathsf{S}_x \\ 0 & 0 & 0 & \mathsf{S}_z^* & \mathsf{S}_y^* & 0 & \mathsf{S}_x^* & \mathsf{M}_8 \end{pmatrix}.$$

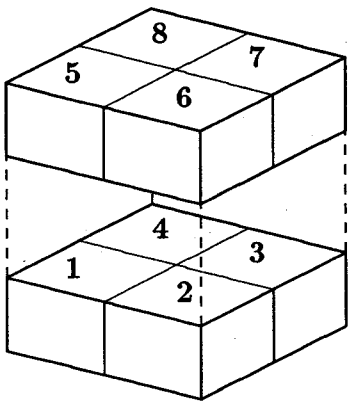

Fig.A1. Configuration of $2 \times 2 \times 2$ superlattice.

Here

$$\mathsf{M}_i = \begin{pmatrix} \mathsf{M}^i_{xyz} & 0 & 0 & 0 \\ 0 & \mathsf{M}^i_{yz} & 0 & 0 \\ 0 & 0 & \mathsf{M}^i_{zx} & 0 \\ 0 & 0 & 0 & \mathsf{M}^i_{xy} \end{pmatrix},$$

$$\mathsf{M}^i_{xyz} = \begin{pmatrix} \varepsilon_{\mathrm{d}\varepsilon} & 0 & \frac{1}{2}V_{\mathrm{pd}\sigma}\mathrm{e}^{-ik_xd} & \frac{1}{2}V_{\mathrm{pd}\sigma}\mathrm{e}^{-ik_yd} & -V_{\mathrm{pd}\sigma}\mathrm{e}^{-ik_zd} \\ 0 & \varepsilon_{\mathrm{d}\varepsilon} & -\frac{\sqrt{3}}{2}V_{\mathrm{pd}\sigma}\mathrm{e}^{-ik_xd} & \frac{\sqrt{3}}{2}V_{\mathrm{pd}\sigma}\mathrm{e}^{-ik_yd} & 0 \\ \frac{1}{2}V_{\mathrm{pd}\sigma}\mathrm{e}^{ik_xd} & -\frac{\sqrt{3}}{2}V_{\mathrm{pd}\sigma}\mathrm{e}^{ik_xd} & \varepsilon_{\mathrm{p}\parallel} & 0 & 0 \\ \frac{1}{2}V_{\mathrm{pd}\sigma}\mathrm{e}^{ik_yd} & \frac{\sqrt{3}}{2}V_{\mathrm{pd}\sigma}\mathrm{e}^{ik_yd} & 0 & \varepsilon_{\mathrm{p}\parallel} & 0 \\ -V_{\mathrm{pd}\sigma}\mathrm{e}^{ik_zd} & 0 & 0 & 0 & \varepsilon_{\mathrm{p}\parallel} \end{pmatrix},$$

$$\mathsf{M}^i_{\alpha\beta} = \begin{pmatrix} 0 & -V_{\mathrm{pd}\pi}\mathrm{e}^{-ik_\beta} & -V_{\mathrm{pd}\pi}\mathrm{e}^{-ik_\alpha} \\ -V_{\mathrm{pd}\pi}\mathrm{e}^{ik_\beta} & 0 & 0 \\ -V_{\mathrm{pd}\pi}\mathrm{e}^{ik_\alpha} & 0 & \end{pmatrix},$$

$\alpha,\ \beta = x,\ y,\ z,$

and nonzero components of S_x, S_y, S_z, which are 14×14 matrices, are given by

$$\mathsf{S}_x(1,3) = \mathsf{S}_x(3,1)^* = -\tfrac{1}{2}V_{\mathrm{pd}\sigma}\mathrm{e}^{-ik_xd}, \qquad \mathsf{S}_x(2,3) = \mathsf{S}_x(3,2)^* = \tfrac{\sqrt{3}}{2}V_{\mathrm{pd}\sigma}\mathrm{e}^{-ik_xd},$$

$$\mathsf{S}_x(6,8) = \mathsf{S}_x(8,6)^* = V_{\mathrm{pd}\pi}\mathrm{e}^{-ik_xd}, \qquad \mathsf{S}_x(12,13) = \mathsf{S}_x(13,12)^* = V_{\mathrm{pd}\pi}\mathrm{e}^{-ik_xd},$$

$$\mathsf{S}_y(1,4) = \mathsf{S}_y(4,1)^* = -\tfrac{1}{2}V_{\mathrm{pd}\sigma}\mathrm{e}^{-ik_yd}, \qquad \mathsf{S}_y(2,4) = \mathsf{S}_y(4,2)^* = -\tfrac{\sqrt{3}}{2}V_{\mathrm{pd}\sigma}\mathrm{e}^{-ik_yd},$$

$$\mathsf{S}_y(6,7) = \mathsf{S}_y(7,6)^* = V_{\mathrm{pd}\pi}\mathrm{e}^{-ik_yd}, \qquad \mathsf{S}_y(9,11) = \mathsf{S}_y(11,9)^* = V_{\mathrm{pd}\pi}\mathrm{e}^{-ik_yd},$$

$$\mathsf{S}_z(1,5) = \mathsf{S}_z(5,1)^* = V_{\mathrm{pd}\sigma}\mathrm{e}^{-ik_zd}, \qquad \mathsf{S}_z(9,10) = \mathsf{S}_z(10,9)^* = V_{\mathrm{pd}\pi}\mathrm{e}^{-ik_zd},$$

$$\mathsf{S}_z(12,14) = \mathsf{S}_z(14,12)^* = V_{\mathrm{pd}\pi}\mathrm{e}^{-ik_zd}.$$

References

1) C. Totsuji and T. Matsubara; Prog. Theor. Phys., **84**, 32 (1990).

2) C. Totsuji and T. Matsubara; J. Phys. Soc. Jpn., **60**, 3549 (1991).

3) C. Totsuji and T. Matsubara; J. Phys. Soc. Jpn., **61**, 1063 (1992).

4) For example, F. Yonezawa and K. Morigaki; Prog. Theor. Phys. Suppl., **53**, 1 (1971).

5) L. F. Mattheiss; Phys. Rev., **B6**, 4718 (1972).

6) T. Wolfram; Phys. Rev. Lett., **30**, 1214 (1972).

7) R. J. Bratton and T. Y. Tien; J. Am. Ceram. Soc., **50**, 90 (1967).